Bulletin of the Seismological Society of America, Vol. 93, No. 3, pp. 1381–1389, June 2003

Short Notes

On the Expected Relationships among Apparent Stress, Static Stress Drop, Effective Shear Fracture Energy, and Efficiency

N. M. Beeler, T.-F. Wong, and S. H. Hickman

Abstract We consider expected relationships between apparent stress τ_a and static stress drop $\Delta\tau_s$ using a standard energy balance and find $\tau_a = \Delta\tau_s(0.5 - \xi)$, where ξ is stress overshoot. A simple implementation of this balance is to assume overshoot is constant; then apparent stress should vary linearly with stress drop, consistent with spectral theories (Brune, 1970) and dynamic crack models (Madariaga, 1976). Normalizing this expression by the static stress drop defines an efficiency $\eta_{sw} = \tau_a/\Delta\tau_s$ as follows from Savage and Wood (1971). We use this measure of efficiency to analyze data from one of a number of observational studies that find apparent stress to increase with seismic moment, namely earthquakes recorded in the Cajon Pass borehole by Abercrombie (1995). Increases in apparent stress with event size could reflect an increase in seismic efficiency; however, η_{sw} for the Cajon earthquakes shows no such increase and is approximately constant over the entire moment range. Thus, apparent stress and stress drop co-vary, as expected from the energy balance at constant overshoot. The median value of η_{sw} for the Cajon earthquakes is four times lower than η_{sw} for laboratory events. Thus, these Cajon-recorded earthquakes have relatively low and approximately constant efficiency. As the energy balance requires $\eta_{sw} = 0.5 - \xi$, overshoot can be estimated directly from the Savage–Wood efficiency; overshoot is positive for Cajon Pass earthquakes. Variations in apparent stress with seismic moment for these earthquakes result primarily from systematic variations in static stress drop with seismic moment and do not require a relative decrease in sliding resistance with increasing event size (dynamic weakening). Based on the comparison of field and lab determinations of the Savage–Wood efficiency, we suggest the criterion $\eta_{sw} > 0.3$ as a test for dynamic weakening in excess of that seen in the lab.

Introduction

Many studies find apparent stress to increase systematically with seismic moment M_0 (Kikuchi and Fukao, 1988; Kanamori *et al.*, 1993; Singh and Ordaz, 1994; Abercrombie, 1995; Mayeda and Walter, 1996; Perez-Campos and Beroza, 2001; Prejean and Ellsworth, 2001). For example, $0.5 < M < 3$ earthquakes recorded at 2.5 km depth in the Cajon Pass, California, borehole have apparent stresses that increase by 2 orders of magnitude with seismic moment from less than 0.01 MPa for the smallest earthquakes to approaching 1 MPa for the largest earthquakes (Fig. 1a) (Abercrombie, 1995). Similarly, for earthquakes recorded in a borehole at Long Valley, California, M 0.5 to M 5 earthquakes have apparent stress that increases from less than 0.01 MPa for the smallest earthquakes to greater than 1 MPa for the largest earthquakes (Prejean and Ellsworth, 2001). Data from broadband recordings in southern California (Kanamori *et al.*, 1993) extend to even higher magnitude ($M > 6$) and show the same general trend (Fig. 1b). Since the apparent stress $\tau_a = \mu E_s/M_0$ (where μ is the shear modulus) corresponds to radiated energy (E_s) per unit area per unit slip, these observations suggest that the source properties of small and large earthquakes are different, so different that the larger earthquakes of the Kanamori *et al.* (1993) data set radiate roughly 1000 times more energy per unit area per unit slip than the small earthquakes of Abercrombie (1995) (Fig. 1b).

Many other seismological observations are not consistent with apparent stress increasing with moment. The large body of observational data suggests that earthquake source processes are independent of event size. For example, most data compilations find that seismic moment and ruptured fault area A are related as $M_0 \propto A^{3/2}$; because, at least for

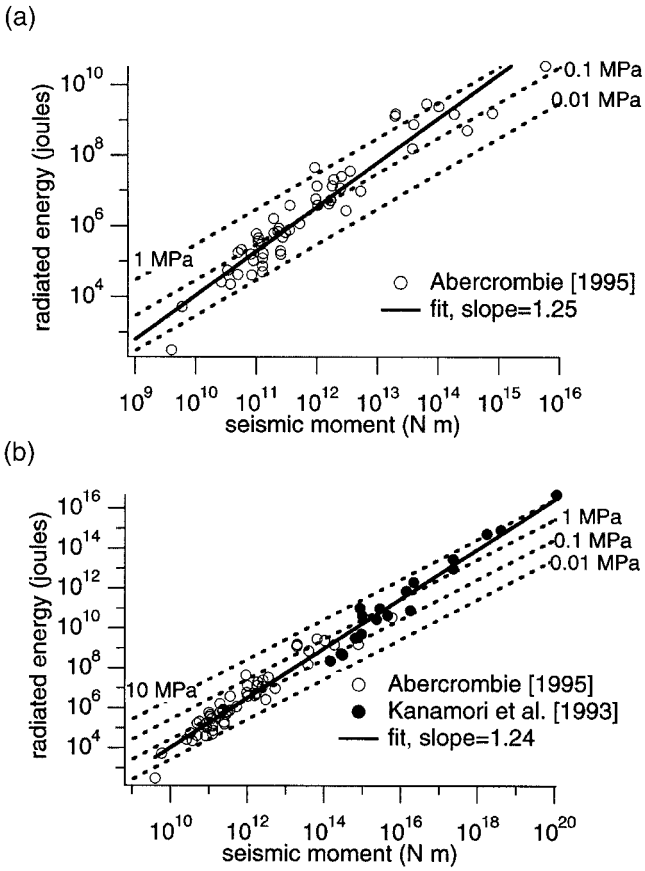

Figure 1. Radiated energy versus moment. (a) Data from Abercrombie (1995). Dashed lines with slope of 1 are lines of constant apparent stress, calculated assuming $\mu = 30{,}000$ MPa. The solid line is a linear least-squares fit to $\log E_a$ versus $\log M_0$, which has slope equal to 1.25. A fit with slope of 1 (not shown) coincides with the dashed 0.1 MPa contour. (b) The data from Abercrombie (1995) shown in panel (a) combined with data of Kanamori *et al.* (1993) that extend to higher seismic moment. Dashed lines are as in panel (a). The solid line is a fit to both data sets and has slope equal to 1.24.

circular ruptures, M_0 varies as $M_0 \propto \Delta\tau_s A^{3/2}$, these observations require stress drop $\Delta\tau_s$ independent of moment over the entire observable magnitude range (Aki, 1967; Kanamori and Anderson, 1975; Hanks, 1977). Increasing apparent stress with moment is also not expected from most earthquake source models. For dynamic crack models, so long as shear fracture energy is negligible or self-similar (e.g., Madariaga, 1976; Boatwright, 1980), apparent stress scales with static stress drop; if stress drop is scale independent as expected, these models yield constant apparent stress. Similarly, spectral theories of the earthquake source require apparent stress to be independent of event size. For example, as shown by Hanks and Thatcher (1972), for the Brune (1970) source model and a circular rupture, apparent stress is entirely independent of event size; the apparent stress associated with the *S* wave is a fixed fraction of the static stress drop.

Under what circumstances would apparent stress increase with seismic moment? Kanamori and Heaton (2000) noted that because of larger displacements, shear heating will be larger for larger earthquakes; they suggested that trends of apparent stress with seismic moment may reflect progressively lower fault shear resistance with increasing earthquake size due to melting or pore fluid pressurization. On the other hand, Ide and Beroza (2001) and Ide *et al.* (2002) believed that trends of increasing apparent stress with moment, at least in some studies, are artifacts due to measurement or analysis errors associated with estimating radiated energy. Bandwidth limitations can lead to underestimated radiated energy, particularly for small earthquakes (Ide and Beroza, 2001), which can have corner frequencies of the same order as the maximum observable frequency. For such earthquakes, to determine apparent stress, some of the radiated energy must be estimated instead of measured, otherwise an artificial size dependence of apparent stress can arise. Other arguments against size scaling of apparent stress were presented by Ide *et al.* (2002). By independently determining site and path effects and a frequency-dependent attenuation, Ide *et al.* (2002) found the Long Valley borehole earthquakes have stress drop and apparent stress that do not vary systematically with seismic moment, contrary to the original analysis of Prejean and Ellsworth (2001).

In this note, we do not attempt to directly determine whether apparent stress does or does not increase with moment, nor do we further discuss the possible analysis and measurement errors of previous studies. Instead, we determine the expected relationships between apparent stress and other seismic source parameters and therefore consider the possible physically based explanations that allow apparent stress to increase with seismic moment, as seemingly is observed. Like Kanamori and Heaton (2000) and Abercrombie and Rice (2001), our approach is based on a simple energy balance similar to that used by Orowan (1960) and Savage and Wood (1971). Our analysis of the energetics of seismic faulting follows from adopting the ratio of the apparent stress to the static stress drop as a quantitative measure of the "efficiency"; this approach is implied by analysis of Savage and Wood (1971). In addition we explicity consider the role of dynamic overshoot in influencing the apparent stress and this ratio. Using this approach, we compare seismological data, particularly data from the Cajon Pass earthquakes of Abercrombie (1995), to laboratory observations where static stress drop and dynamic strength are measured directly. Our comparison and analysis suggest that variations in apparent stress with seismic moment for the Cajon Pass data result primarily from variations in static stress drop with seismic moment and that overshoot is positive for these earthquakes. If in addition we explicitly analyze the contribution of the fracture energy, then variations in apparent stress can arise from trade-offs between fracture energy and overshoot behavior during dynamic rupture.

Energy Balance

In this section we analyze, in the simplest and most general way we could think of, the factors that determine the size of apparent stress during earthquake stress drop. Symbols used in our analysis, and their definitions, are listed in Table 1. We first consider the total energy released by an earthquake and then develop an expression for the fraction that is radiated. The total energy released during seismic stress drop is $W = \bar{\tau}Ad$, where A is the ruptured fault area, d is the seismic slip spatially averaged over the rupture surface area, and $\bar{\tau}$ is the spatially averaged stress during the earthquake. The spatially averaged beginning τ_0 and ending τ_1 stresses are related to $\bar{\tau}$ by $\bar{\tau} = (\tau_0 + \tau_1)/2$ and the static stress drop $\Delta\tau_s$ to the beginning and ending stresses by $\tau_s = \tau_0 - \tau_1$. Note that this static stress drop and the dynamic stress drop $\tau_d = \tau_0 - \tau_f$ are defined with reference to τ_0 (Fig. 2), which corresponds to the initial stress. In some treatments, particularly those that consider fracture energy, initial stress differs from the peak or yield stress τ_y, defining a "strength excess" $\tau_y - \tau_0$, which is an important parameter in determining slip and rupture speeds during dynamic rupture (e.g., Andrews, 1985). We do not explicitly consider dynamic rupture in this article. The yield stress does not appear in the energy balance approach we use in this article, even when we consider the fracture energy explicitly in a later section; as seismologic observations seem to provide no constraint on the yield stress or the strength excess (Guatteri and Spudich, 2000), we ignore the excess in the remainder of this article.

The total energy released per unit rupture area can be depicted schematically in a plot of stress versus displacement (Fig. 2). With reference to Figure 2a, the total energy released, here having units of joules per square meter (equivalently pascal meters), is the area under the heavy dashed line. All of our subsequent analyses can be derived graphically from such stress versus displacement diagrams. The total energy released during seismic stress drop can be alternatively expressed as $W = \bar{\tau}M_0/\mu$, where μ is the shear modulus and M_0 is the seismic moment ($M_0 = \mu dA$). This total energy W is balanced by the sum of energy that is dissipated by frictional heating and fracture in the fault zone $E_F = \bar{\tau}_k M_0/\mu$ and the radiated energy $E_s = M_0\tau_a/\mu$, that is,

$$W = E_F + E_S. \tag{1a}$$

Here $\bar{\tau}_k$ and τ_a are the spatially and displacement-averaged fault shear resistance and apparent stress, respectively. When normalized by the fault area and average slip, the energies in equation (1a) have dimensions of stress, i.e.,

$$\bar{\tau} = \bar{\tau}_k + \tau_a. \tag{1b}$$

Three examples of possible relative sizes of the terms in equation (1b) are depicted in Figure 2. Due to inertial effects, the final stress τ_1 may be different from the average resisting stress $\bar{\tau}_k$, and this overshoot phenomenon will be explicitly considered here. In many dynamic crack models, the overshoot $\bar{\tau}_k - \tau_1$ is positive (e.g., Madariaga, 1976), but if local fault healing induces dynamic slip termination then the overshoot can be negative (e.g., Ide, 2002).

Table 1
Symbols Used in This Study and Their Definitions

μ	Shear modulus
E_s	Radiated energy
A	Fault area ruptured during seismic slip
d	Seismic slip spatially averaged over the seismic rupture
$\bar{\tau}$	Displacement-averaged shear stress spatially averaged over the seismic rupture
W	Total energy released during seismic slip, $W = \bar{\tau}Ad$
E_F	Sum of energy dissipated by frictional sliding and stored in surface energy during seismic slip, $E_F = \bar{\tau}_k M_0/\mu$
τ_a	Apparent stress, $\tau_a = \mu E_s/M_0$
M_0	Seismic moment, $M_0 = \mu dA$
τ_0	Initial stress spatially averaged over the seismic rupture
τ_y	Yield stress or peak stress spatially averaged over the seismic rupture
τ_1	Stress at the cessation of seismic slip spatially averaged over the seismic rupture
$\Delta\tau_s$	Static stress drop spatially averaged over the seismic rupture, $\Delta\tau_s = \tau_0 - \tau_1$
$\Delta\tau_d$	Dynamic stress drop spatially averaged over the seismic rupture, $\Delta\tau_d = \tau_0 - \tau_f$
$\bar{\tau}_k$	Displacement-averaged shear strength spatially averaged over the seismic rupture
ξ	A measure of overshoot, $\xi = (\bar{\tau}_k - \tau_1)/\Delta\tau_s$
η_{sw}	Savage–Wood efficiency, $\eta_{sw} = \tau_a/\Delta\tau_s$
τ_f	Residual fault strength
G_e	Effective shear fracture energy, $G_e = (\bar{\tau}_k - \tau_f)d$
τ_c	Fracture stress, $\tau_c = \bar{\tau}_k - \tau_f = G_c/d$
ξ_*	A measure of overshoot specific to linear slip-weakening fault strength $\xi_* = (\tau_f - \tau_1)/\Delta\tau_s$
η_{τ_c}	Fracture efficiency, $\eta_{\tau_c} = \tau_c/\Delta\tau_s$
η_R	Radiation efficiency, $\eta_R = 2\tau_a/\Delta\tau_s$

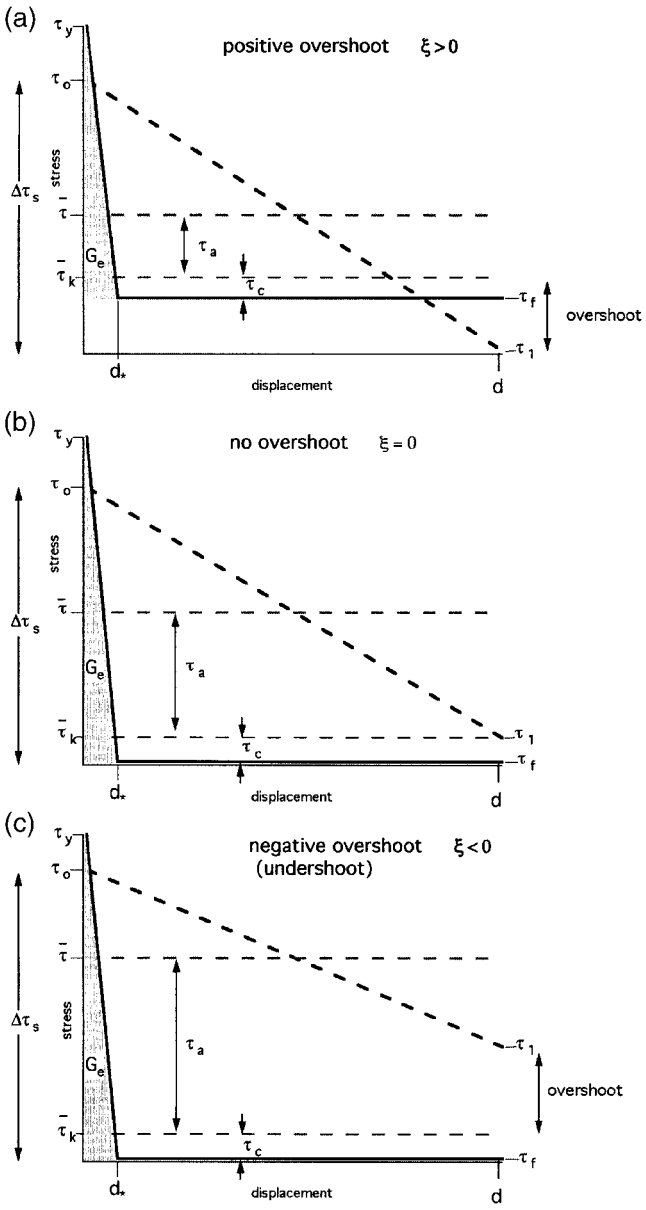

Figure 2. Schematic diagrams showing the energy per unit fault area (e.g., joules per meter squared) released during an earthquake. This energy per fault area can be expressed equivalently as stress times displacement; stress and displacement are the axes of the figures. Thus, the energy/fault area corresponds to an area on the plot (e.g., the shaded region in each diagram that corresponds to fracture energy). The total energy released expressed in terms of spatially averaged stress units is $\bar{\tau} = \bar{\tau}_k + \tau_a$, where $\bar{\tau}$ is the mean shear stress, $\bar{\tau}_k$ is the displacement-averaged strength, and τ_a is the apparent stress. Strength (heavy black line) is shown as a function of fault displacement during stress drop. Stress (heavy black dashed line) is also shown; the area under this stress line is the total energy released per unit fault area. The dynamic overshoot is $\xi = (\bar{\tau}_k - \tau_1)/(\tau_0 - \tau_1)$. The lower limit of stress is generally thought to not coincide with zero; however, this lower limit is not constrained by seismic observations, that is, for earthquakes the stress drop $\Delta\tau_s$ is known and $\bar{\tau}$ is unknown (e.g., Randall, 1972). In these three examples, the static stress drop is fixed, while the effective shear fracture energy G_e (stippled), apparent stress $\tau_a = \bar{\tau} - \bar{\tau}_k$, and fracture stress $\tau_c = \bar{\tau}_k - \tau_f$ are nonzero. (a) In this example, the dynamic strength is similar in size to the mean stress but is somewhat smaller than the final stress, leading to positive overshoot, $\xi = 0.27$, and a small Savage–Wood efficiency, $\eta_{sw} = \tau_a/\Delta\tau_s = 0.23$. This case is consistent with laboratory observations of stick-slip faulting (e.g., Okubo and Dieterich, 1984) and elastodynamic fracture models of earthquake stress drop (see summary in Kostrov and Das [1988]). (b) In this second example, the average dynamic strength is equal to the final stress so there is no overshoot, $\xi = 0$, leading to higher efficiency, $\eta_{sw} = 0.5$, than in panel (a). (c) In this final example, the average dynamic strength is much lower than the final stress; this is a case of dynamic weakening greatly exceeding that seen in laboratory experiments (Fig. 2a), as might be caused by shear melting or pore fluid pressurization with self-healing rupture. Overshoot is negative, $\xi = -0.5$, and the Savage–Wood efficiency is very high, $\eta_{sw} = 1$.

If we follow McGarr (1999) to define a stress overshoot $\xi = (\bar{\tau}_k - \tau_1)/\Delta\tau_s$ that is normalized by the static stress drop $\Delta\tau_s$, then the apparent stress can be written as

$$\tau_a = \Delta\tau_s(0.5 - \xi). \quad (1c)$$

Note that overshoot in equation (1c) is bounded ($\xi < 0.5$). As equation (1c) implies, observed variations of apparent stress with seismic moment result from trade-off between static stress drop and overshoot. A simple implementation of this balance is to assume constant overshoot. In that special case, apparent stress should vary linearly with stress drop, a result that is consistent with spectral theories (Brune, 1970) and dynamic crack models (Madariaga, 1976). In the following, we allow for the general case where stress drop and overshoot are both allowed to vary with moment.

Analysis

In this section, we show that a simple measure of efficiency, which follows from equation (1c), provides a useful context for analyzing source properties that might scale with event size. The conventional seismic efficiency, the ratio of the radiated energy to the total energy released, or equivalently the ratio of apparent stress to mean stress, has been estimated for earthquakes, for example by Savage and Wood (1971) and McGarr (1994, 1999). However, $\bar{\tau}$ is usually not well known and cannot be determined from seismic data, making η generally difficult to estimate reliably. A different measure of efficiency, the ratio of apparent stress to the static stress drop

$$\eta_{sw} = \tau_a/\Delta\tau_s, \quad (2)$$

is more easily determined. Savage and Wood (1971) first considered bounds on apparent stress relative to the size of the static stress drop, thus we refer to ratio (2) as the Savage–Wood efficiency. A quantity equal to twice equation (2), called the radiation efficiency was considered by Husseni and Randall (1976) and Husseni (1977). The radiation efficiency is simply the percentage of energy associated with the stress drop that is radiated; the Savage–Wood efficiency (equation 2) is one-half the radiation efficiency (see Discussion). Example possible values of equation (2) are shown in Figure 2; also see Ide (2002).

A simple relation for η_{sw} follows from equation (1c)

$$\eta_{sw} = 0.5 - \xi. \tag{3}$$

As with η_{sw}, the overshoot ξ is a stress measure normalized by the static stress drop. The overshoot measures whether the static stress drop is larger ($\xi > 0$; Fig. 2a) or smaller ($\xi < 0$; Fig. 2c) than the dynamic stress drop $\tau_0 - \bar{\tau}_k$. Alternatively, and more to the point of our analysis, overshoot measures how large the dynamic strength $\bar{\tau}_k$ is relative to the residual stress τ_1; high values of overshoot reflect high dynamic strength relative to the stress level (Fig. 2a), and low values of ξ reflect low relative strength (Fig. 2c). Thus, equation (3) equates the Savage–Wood efficiency (known from apparent stress and static stress drop) to the relative dynamic strength (ξ).

Lines of constant overshoot are straight with zero slope in a plot of η_{sw} versus seismic moment; these are lines of "self-similarity" of efficiency (Fig. 3). In the remainder of this article, we examine η_{sw} from τ_a and $\Delta\tau_s$ determined in previously published studies. We consider these data in the context of equation (3) without account of possible measurement or analysis errors associated with the data. For the Cajon Pass earthquakes, η_{sw} calculated from τ_a and $\Delta\tau_s$ tabulated by Abercrombie (1995) does not depend systematically on seismic moment and has a median value of $\eta_{sw} = 0.053$, which is nearly four times lower than the median value for laboratory measurements (e.g., 0.22, Lockner and Okubo [1983]) (Fig. 3). Observations from mining-induced earthquakes (McGarr, 1991) are consistent with the lab data (McGarr, 1994) (Fig. 3). The difference between the lab and Cajon η_{sw} can only be accounted for if the Cajon earthquakes have higher overshoot (relatively high dynamic strength) than the lab observations.

Kanamori and Heaton (2000) argued that the largest earthquakes in the Kanamori *et al.* (1993) data set show evidence of decreasing dynamic fault strength (dynamic weakening) with increasing seismic moment because the largest earthquakes have the highest apparent stress. Under these circumstances, if the static stress drop were constant, increasing apparent stress would correspond to decreasing overshoot. Unfortunately, the Savage–Wood efficiency for the complete Kanamori *et al.* (1993) data set cannot be estimated from their published information, and we are only able to plot a few of their larger earthquakes in Figure 3;

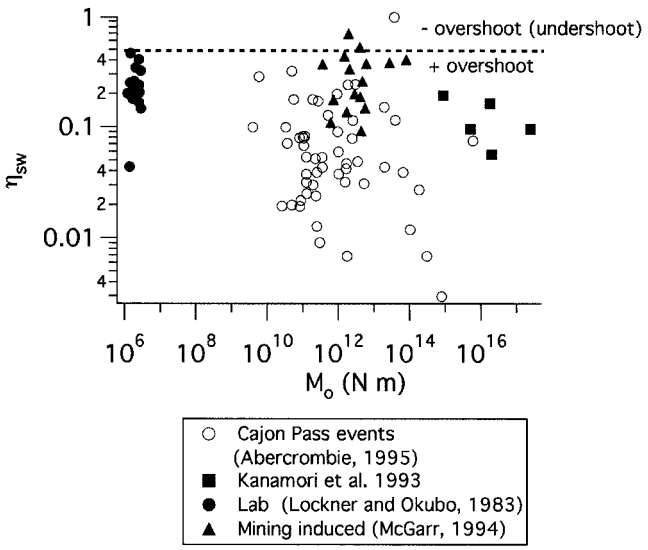

Figure 3. The Savage–Wood efficiency $\eta_{sw} = \tau_a/\Delta\tau_s$ versus seismic moment for three seismological data sets and one set of lab observations. The open symbols are data from earthquakes recorded at 2.5 km depth at Cajon Pass (Abercrombie, 1995). The stress drop and apparent stress used in determining η_{sw} are inferred by spectral modeling of the observations; these are model 2 of Abercrombie (1995). Also shown are earthquakes in southern California from the study of Kanamori *et al.* (1993) (solid squares). The apparent stresses from this data set are the ratio E_s/M_0 from table 2 in Kanamori *et al.* (1993), assuming a shear modulus of 30,000 MPa. The corresponding static stress drops of Kanamori *et al.* (1993) were estimated using pulse width t_d data from table 3 of Kanamori *et al.* (1993) and the relation of Cohn *et al.* (1982), $\Delta\tau_s$ (bar) = M_0 (dyne cm) [$5.69 \times 10^{-8}/t_d$ (sec)] (see also figure 9 of Kanamori *et al.* [1993]). Tabulated data from mining induced earthquakes (McGarr, 1994) (solid triangles) and from laboratory stress drops (solid circles) (Lockner and Okubo, 1983) are shown for comparison. The dashed line, which corresponds to equation (2) with zero overshoot ξ, separates $\xi < 0$ (undershoot) from $\xi > 0$ (overshoot).

still, values of η_{sw} similar to the Cajon data are found for these large earthquakes (Fig. 3). Based on these few points from Kanamori *et al.* (1993) and our analysis of the Cajon earthquakes, we find no evidence for systematic decreases in dynamic strength causing increasing apparent stress with seismic moment. This is well illustrated by a plot of apparent stress versus static stress drop (Fig. 4). Here, with reference to equation (1c), lines of constant overshoot have slope of 1. A fit to the Cajon Pass data shows a slope lower than 1, corresponding to increasing overshoot (an *increase* in relative dynamic strength). In summary, we conclude that the trend of increasing apparent stress with seismic moment in this particular Cajon Pass data set is not consistent with the largest earthquakes having excess radiated energy. Instead, at least compared to laboratory and mining observations, the Cajon Pass earthquakes have low efficiency and high overshoot.

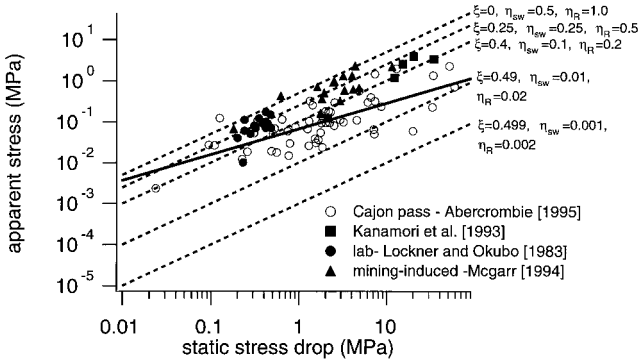

Figure 4. Apparent stress versus static stress drop for three seismological data sets and one set of lab observations. Symbols are as in Figure 3. Contours of constant overshoot have a slope of 1 on this plot (see equation lc); the contours shown correspond to the labeled values of overshoot. The solid line is a fit to the Cajon Pass data of Abercrombie (1995) (open symbols), with a slope of 0.63.

Because η_{sw} is essentially independent of seismic moment (Fig. 3) and apparent stress increases with seismic moment (Fig. 1), static stress drop co-varies with apparent stress for the Cajon earthquakes (Fig. 4). This relationship, clearly noted by Abercrombie (1995) (see her figure 12), is somewhat weaker than expected were overshoot constant (equation 1c), but not dramatically so. Our interpretation of the data is that the variation of apparent stress with moment results from systematic variation of stress drop with event size and that there is a weak increase in overshoot with moment. According to this interpretation, the data are not consistent with dramatic changes in source physics with event size. Based on the energy balance derived proportionality between stress drop and apparent stress (equation 1c) and the many source models that are consistent with this proportionality (e.g., Hanks and Thatcher, 1972), we suggest that systematic, orders-of-magnitude variation of apparent stress with event size in observational data sets, whether real or artifact, result largely from similar variations of stress drop with event size.

Discussion

The apparent stress is the displacement-averaged value of the radiated resistance τ_R; for example, in simple models (Rice, 1993) the dynamic value of radiated resistance is $\tau_R(\delta) = \chi V(\delta)$, where V is slip velocity and χ is half the ratio of the shear modulus to the shear-wave speed. In general, the apparent stress is proportional to the spatially and displacement-averaged slip velocity (McGarr and Fletcher, 2001, 2002). The small values of η_{sw} for earthquakes in the observational studies (Fig. 3) imply slip velocities that are proportionately smaller than for lab and mining-induced earthquakes of equivalent size; similarly, the observed low values of τ_a imply lower rupture velocity and longer event duration. We view these implied low values of slip velocity as an expected consequence of low efficiency, but, as our analysis does not consider rupture dynamics, we cannot comment quantitatively on expected relationships between apparent stress, shear fracture energy, slip velocity, and rupture velocity.

Estimates of the Savage–Wood efficiency may have significant uncertainties because estimated static stress drop is model dependent (McGarr, 1994) and estimates of apparent stress are subject to errors from attenuation and bandwidth limitations (e.g., Ide and Beroza, 2001; Ide *et al.*, 2002). Note also that we have used data from previously published studies, have assumed that these data are accurate, and have not considered the formal uncertainties associated with the data. If these data are in error, as Ide and Beroza (2001) have suggested for the smallest events in the Abercrombie (1995) data set, or uncertain, those errors and uncertainites are inherent in our data analysis. However, reliable estimates of η_{sw} may allow interpretable constraints to be placed on dynamic fault strength. For laboratory and small induced earthquake observations of stress drop (Wong, 1986; McGarr, 1994, 1999), fault strength is in accord with Byerlee's law (Byerlee, 1978), overshoot is positive and in the range $\xi = 0.2$–0.3 (McGarr, 1994, 1999), and typically $\eta_{sw} < 0.30$. This case is schematically depicted in Figure 2a. In contrast, for dynamic weakening in excess of that seen in the lab, more energy would be radiated relative to the sum of energy dissipated by friction and that stored in fracture energy, for example, as shown in Figure 2b. In instances of pronounced dynamic weakening, the shear resistance could drop dramatically during stress drop; if the dynamic stress drop exceeds the static stress drop, then $\xi < 0$ (undershoot) (Fig. 2c). In the most extreme case of dynamic weakening, for example, due to pore fluid pressurization or frictional melting, the shear resistance falls to zero, all the energy is radiated, $\eta = 1$, $\eta_{sw} = \tau_0/\Delta\tau_s$, and the Savage–Wood efficiency could easily exceed 1. We suggest that evidence of dynamic weakening might be inferred simply from η_{sw} exceeding lab-like values that result at dry conditions where thermal pressurization of pore fluids is impossible and where fault displacements and fault normal stress are far too small to lead to shear melting. Using the criterion $\eta_{sw} > 0.3$, there is no clear evidence for dynamic weakening in excess of that seen in the lab in any of the data sets we examined (Fig. 3).

Fracture Energy, Fracture Stress, and Efficiency

Experimental evidence shows that a slip-weakening relation well describes changes of strength during fracture of intact rock and changes in strength during seismic earthquakes on preexisting faults (e.g., Wong, 1986). Slip-weakening fault strength has a well-defined effective shear fracture energy, and for fracture-mechanics-based models of earthquake rupture, this fracture energy in part determines the speed of rupture propagation (see summary in Kostrov and Das, 1988) and thereby influences the radiated energy (e.g., Madariaga, 1976; Boatwright, 1980). Therefore it is

useful to reconsider the energy balance (equation 1a) and the efficiency for a slip-weakening fault, keeping in mind that conclusions drawn from the following analysis are model dependent. We assume fault strength at the onset of dynamic slip drops from the peak strength τ_y with displacement over a characteristic distance d^* and remains constant with subsequent slip (Ida, 1972; Palmer and Rice, 1973) (Fig. 2). With this slip-weakening relationship, the residual shear strength is τ_f, defining an effective shear fracture energy associated with the strength loss $G_e = (\bar{\tau}_k - \tau_f)d$. The fracture stress, the stress measure of effective shear fracture energy, is $\tau_c = \bar{\tau}_k - \tau_f = G_e/d$. Thus for this general slip weakening, equation (1b) can be recast as

$$\bar{\tau} = \tau_f + \tau_c + \tau_a. \tag{4a}$$

Solving equation (4a) for the apparent stress in terms of the static stress drop $\Delta\tau_s$, the fracture stress, and overshoot $\xi_* = (\tau_f - \tau_0)/\Delta\tau_s$, we find

$$\tau_a = \Delta\tau_s\,(0.5 - \xi_*) - \tau_c. \tag{4b}$$

Note that overshoot as used in equation (4b) is bounded ($\xi_* < 0.5$) and that this measure of overshoot is defined with respect to τ_f, similar to the approach commonly used in crack models (e.g., Madariaga, 1976). In contrast, ξ is defined with respect to $\bar{\tau}_k$; to equate these two measures of overshoot, we have $\xi = \xi_* + \tau_c/\Delta\tau_s$. A relation for η_{sw} follows from normalizing equation (4b) by the static stress drop

$$\eta_{sw} = 0.5 - \xi_* - \eta_{\tau_c}, \tag{4c}$$

where $\eta_{\tau_c} = \tau_c/\Delta\tau_s$ is the "fracture efficiency", one-half the percentage of energy associated with the static stress drop that is dissipated by fracture and friction during the strength drop. Thus, for slip weakening (equation 4c), the known Savage–Wood efficiency must be balanced by contributions due to the residual dynamic strength (ξ_*) and the shear fracture energy (η_{τ_c}).

Previously, relationships between radiated and fracture energy have been addressed using the radiation efficiency η_R, originally defined by Husseni and Randall (1976) and Husseni (1977) (also see Randall, 1972). The radiation efficiency η_R is the ratio of radiated to available energy. Recent analyses relating radiation efficiency to radiated and fracture energy (Venkataraman and Kanamori, 2002) and recent general analysis of fracture energy (Abercrombie and Rice, 2001) repeat an arbitrary assumption of Husseni (1977) and Orowan (1960) that the static stress drop is equal to the dynamic stress drop, that is, no dynamic overshoot. For this special case there is a simple relation between efficiency and the radiated and fracture energies; the energy associated with the static stress drop $\Delta\tau_s M_0/(2\mu)$ is exactly partitioned between radiated and fracture energy and the radiation efficiency is $\eta_R = E_S/(E_S + G_e A) = 2\tau_a/\Delta\tau_s$ (Venkataraman and Kanamori, 2002). However, if instead overshoot is nonzero, then $E_S/(E_S + G_e A) \neq 2\tau_a/\Delta\tau_s$. So that radiation efficiency is unambiguously defined in cases of non-zero overshoot, we propose that η_R be generally defined as the ratio of radiated energy to energy associated with the stress drop $\eta_R = 2\tau_a/\Delta\tau_s$. Thus, radiation efficiency is twice the Savage–Wood efficiency.

A number of previous theoretical and observational studies (e.g., Madariaga, 1976; McGarr, 1999; Ide, 2002) suggest that overshoot is nonzero and we are not certain that the sign and magnitude of overshoot are constant with moment. Therefore, in the following we consider efficiency, fracture energy and radiated energy of earthquakes for the general case represented by equation (4c).

If interpreted using the slip-weakening fault strength, the difference between the lab and Cajon Pass η_{sw} (Fig. 3) can only be accounted for if the Cajon earthquakes have some combination of higher overshoot (relatively high dynamic strength) and higher fracture efficiency than the lab observations. For example, in reference to equation (4c), if $\xi_* = 0$, then the Cajon pass earthquakes would have an extremely high median fracture efficiency $\eta_{\tau_c} = 0.45$, corresponding to 90% of the energy associated with the stress drop. To our knowledge, there is no experimental or theoretical evidence to support values of fracture efficiency anywhere near this high for seismic earthquakes. In the case of laboratory observations, fracture energy is observed to be a small fraction of the energy associated with stress drop (e.g., Okubo and Dieterich, 1984). For earthquakes, usually the contribution of fracture energy to the earthquake energy budget is assumed to be very small, and quite often fracture energy is ignored entirely (e.g., Kanamori and Heaton, 2000). Still, the relative size of fracture energy for earthquakes could be large; recent estimates from dynamic modeling produce fracture energy that is 60% of the energy associated with the stress drop ($\eta_{\tau_c} = 0.30$) (Favreau and Archeluta, 2002), and the size of the fracture efficiency for earthquakes remains an open question.

On the other hand, the maximum possible overshoot is $\xi_* = 0.5$; if the fracture efficiency is assumed to be zero, then the Cajon Pass earthquakes would have nearly complete overshoot, $\xi_* = 0.45$. We are aware of no experimental, theoretical, or observational evidence that supports overshoot this high. For example, dynamic fracture models typically have $\xi_* \approx 0.1$–0.2 (e.g., Kostrov and Das, 1988); the slider block calculations of Beeler (2001) show that even if the fracture stress is zero, overshoot will not greatly exceed that in laboratory observations, where typically $\xi_* \approx 0.27$ (McGarr, 1994). From these considerations, we expect that these Cajon Pass earthquakes have some combination of positive overshoot and large fracture efficiency relative to lab observations. Although fracture efficiency and ξ_* are not distinguished by our analysis, their sum for the Cajon earthquakes is ~0.45. Because at 0.053 the Savage–Wood efficiency is much lower than the sum of ξ_* and η_{τ_c}, likely for these earthquakes the fracture efficiency is of the same mag-

nitude as the Savage–Wood efficiency, in which case fracture energy is of the same magnitude as radiated energy.

Conclusions

For earthquakes recorded in the Cajon Pass borehole ($M < 3$) (Abercrombie, 1995), apparent stress increases with moment, but the Savage–Wood efficiency $\eta_{sw} = \tau_a/\Delta\tau_s$ is approximately constant and roughly four times smaller than seen in lab data. Thus, these earthquakes have low and approximately scale-independent efficiency. Variations in apparent stress with seismic moment for these earthquakes result primarily from systematic variations in static stress drop with seismic moment and do not require increases in severity of dynamic weakening with moment. Likely, overshoot is positive and the fracture energy is not negligible. We suggest comparison of field and lab determinations of the Savage–Wood efficiency as a test for dynamic weakening in excess of that seen in laboratory experiments.

Acknowledgments

Rachel Abercrombie provided the data from the Cajon Pass recorded earthquakes and explanations of her unpublished analysis of earthquake source properties and fracture energy. Comments by and discussions with B. Ellsworth, J. Savage, S. Ide, and particularly A. McGarr, T. Hanks, P. Spudich, R. Archuleta, and R. Abercrombie are gratefully acknowledged.

References

Abercrombie, R. E. (1995). Earthquake source scaling relationships from −1 to 5 M_L using seismograms recorded at 2.5 km depth, *J. Geophys. Res.* **100,** 24,015–24,036.

Abercrombie, R. E., and J. R. Rice (2001). Small earthquake scaling revisited: can it constrain slip weakening? *EOS* **82,** F843.

Aki, K. (1967). Scaling law of seismic spectrum, *Bull. Seism. Soc. Am.* **72,** 1217–1231.

Andrews, D. J. (1985). Dynamic plane-strain shear rupture with a slip-weakening friction law calculated by a boundary integral method, *Bull. Seism. Soc. Am.* **75,** 1–21.

Beeler, N. M. (2001). Stress drop with constant, scale independent seismic efficiency and overshoot, *Geophys. Res. Lett.* **28,** 3353–3356.

Boatwright, J. (1980). A spectral theory for circular seismic sources: simple estimates of source dimension, dynamic stress drop and radiated seismic energy, *Bull. Seism. Soc. Am.* **70,** 1–27.

Brune, J. N. (1970). Tectonic stress and the spectra of seismic shear waves from earthquakes, *J. Geophys. Res.* **75,** 4997–5009.

Byerlee, J. D. (1978). Friction of rocks, *Pure Appl. Geophys.* **116,** 615–625.

Cohn, S. N., T. L. Hong, and D. V. Helmberger (1982). The Oroville earthquakes: a study of source characteristics and site effects, *J. Geophys. Res.* **87,** 4585–4594.

Favreau, P., and R. J. Archuleta (2002). Direct seismic energy modeling and application to the 1979 Imperial valley earthquake, *Geophys. Res. Lett.* **30,** 1198–1201.

Guatteri, P., and P. Spudich (2000). What can strong motion data tell us about slip-weakening fault friction laws? *Bull. Seism. Soc. Am.* **90,** 98–116.

Hanks, T. C. (1977). Earthquake stress drops, ambient tectonic stresses, and stresses that drive plate motions, *Pure Appl. Geophys.* **115,** 441–458.

Hanks, T., and W. Thatcher (1972). Graphical representation of seismic source parameters, *J. Geophys. Res.* **77,** 4393–4405.

Husseini, M. I. (1977). Energy balance for motion along a fault, *Geophys. J. Astr. Soc.* **49,** 699–714.

Husseini, M. I., and M. J. Randall (1976). Rupture velocity and radiation efficiency, *Bull. Seism. Soc. Am.* **66,** 1173–1187.

Ida, Y. (1972). Coheseive forces across the tip of a longitudinal-shear crack and Griffith's specific surface energy, *J. Geophys. Res.* **77,** 3796–3805.

Ide, S. (2002). Estimation of radiated energy of finite source models, *Bull. Seism. Soc. Am.* **92,** 2994–3005.

Ide, S., and G. C. Beroza (2001). Does apparent stress vary with earthquake size? *Geophys. Res. Lett.* **28,** 3349–3352.

Ide, S., G. C. Beroza, S. G. Prejean, and W. L. Ellsworth (2002). Earthquake scaling down to M1 observed at 2 km depth in the Long Valley Caldera, California, *J. Geophys. Res.* (submitted).

Kanamori, H., and D. L. Anderson (1975). Theoretical basis of some empirical relations in seismology, *Bull. Seism. Soc. Am.* **65,** 1073–1095.

Kanamori, H., and T. H. Heaton (2000). Microscopic and macroscopic physics of earthquakes, in *Geocomplexity and the Physics of Earthquakes*, J. Rundle, D. L. Turcotte, and W. Klein (Editors), American Geophysical Monograph 120, 147–155.

Kanamori, H., E. Hauksson, L. K. Hutton, and L. M. Jones (1993). Determination of earthquake energy release and M_L using terrascope, *Bull. Seism. Soc. Am.* **83,** 330–346.

Kikuchi, M., and Y. Fukao (1988). Seismic wave energy inferred from long-period body wave inversion, *Bull. Seism. Soc. Am.* **78,** 1707–1724.

Kostrov, B. V., and S. Das (1988). *Principles of Earthquake Source Mechanics*, Cambridge U Press, New York.

Lockner, D. A., and P. G. Okubo (1983). Measurements of frictional heating in granite, *J. Geophys. Res.* **88,** 4313–4320.

Madariaga, R. (1976). Dynamics of an expanding circular fault, *Bull. Seism. Soc. Am.* **66,** 639–666.

Mayeda, K., and W. R. Walter (1996). Moment, energy, stress drop, and source spectra of western United States earthquakes from regional coda envelopes, *J. Geophys. Res.* **101,** 11,195–11,208.

McGarr, A. (1991). Observations constraining near source ground motion estimated from locally recorded seismograms, *J. Geophys. Res.* **96,** 16,495–16,508.

McGarr, A. (1994). Some comparisons between mining-induced and laboratory earthquakes, *Pure Appl. Geophys.* **142,** 467–489.

McGarr, A. (1999). On relating apparent stress to the stress causing earthquake fault slip, *J. Geophys. Res.* **104,** 3003–3011.

McGarr, A., and J. B. Fletcher (2001). A method for mapping apparent stress and energy radiation applied to the 1944 Northridge earthquake fault zone—revisited, *Geophys. Res. Lett.* **28,** 3529–2932.

McGarr, A., and J. B. Fletcher (2002). Mapping apparent stress and energy radiation over fault zones of major earthquakes, *Bull. Seism. Soc. Am.* **92,** 1633–1646.

Okubo, P. G., and J. H. Dieterich (1984). Effects of physical fault properties on frictional instabilities produced on simulated faults, *J. Geophys. Res.* **89,** 5817–5827.

Orowan, E. (1960). Mechanism of seismic faulting in rock deformation, Geol. Soc. Am. Memoir, Vol. 79, 323–345.

Palmer, A. C., and J. R. Rice (1973). The growth of slip surfaces in the progressive failure of over-consolidated clay, *Proc. R. Soc. London A* **332,** 527–548.

Perez-Campos, X., and G. C. Beroza (2001). An apparent mechanism dependence of radiated seismic energy, *J. Geophys. Res.* **106,** 11,127–11,136.

Prejean, S., and W. L. Ellsworth (2001). Observations of earthquake source parameters at 2 km depth in the Long Valley caldera, eastern California, *Bull. Seism. Soc. Am.* **91,** 165–177.

Randall, M. J. (1972). Stress drop and the ratio of seismic energy to moment, *J. Geophys. Res.* **77,** 969–970.

Rice, J. R. (1993). Spatio-temporal complexity of slip on a fault, *J. Geophys. Res.* **98,** 9885–9907.

Savage J. C., and M. D. Wood (1971). The relation between apparent stress and stress drop, *Bull. Seism. Soc. Am.* **61,** 1381–1388.

Singh, S. K., and M. Ordaz (1994). Seismic energy release in Mexican subduction zone earthquakes, *Bull. Seism. Soc. Am.* **84,** 1533–1550.

Venkataraman, A., and H. Kanamori (2002). Using macroscopic seismological parameters to understand the dynamics of faulting, *EOS* **83,** F1030.

Wong, T.-F. (1986). On the normal stress dependence of the shear fracture energy, in *Earthquake Source Mechanics*, S. Das, J. Boatwright, and C. H. Scholz (Editors), American Geophysical Monograph 37, 1–11.

U.S. Geological Survey, MS 977
345 Middlefield Rd.
Menlo Park, California 94025
(N.M.B., S.H.H.)

Dept. of Geosciences
ESS Building
State University of New York Stony Brook
Stony Brook, New York, 11794-2100
(T.-F.W.)

Manuscript received 30 July 2002.